FULL PAPER

Flocculated CNTs

small
method

www.small-methods.com

Check for
updates

Enhanced Process Integration and Device Performance of Carbon Nanotubes via Flocculation

Theodore Z. Gao, Ting Lei, Francisco Molina-Lopez, and Zhenan Bao*

Polymer sorting is a promising strategy for purifying semiconducting carbon nanotubes (CNTs), offering high selectivity and yield, in addition to low cost and scalability. However, sorting conditions that maximize the yield lead to CNT dispersions with significant amounts of excess sorting polymer. This has undesirable implications for CNT device performance, such as decreased charge carrier mobility and on–off ratio. Here, a method for removing excess sorting polymer based on flocculation is demonstrated. This approach is broadly applicable to various sorting polymers and facilitates recycling of the sorting polymer. In addition, devices made with flocculated CNTs exhibit improved performance and require minimal post-processing steps. Flocculation was found to be particularly effective for inkjet-printed CNT transistors on SiO$_2$, producing devices with mobilities ≈10 cm^2 V^{-1} s^{-1} and on–off ratios ≈10^6. These results show that flocculation is a facile approach to improving the process integration and device performance of polymer-sorted CNTs.

1. Introduction

Semiconducting carbon nanotubes (CNTs) are a promising material for flexible and stretchable electronics due to their high intrinsic charge carrier mobilities, solution-processability, and robust mechanical properties.[1–7] However, bulk-scale production of CNTs creates a mixture of semiconducting and metallic CNTs, limiting their technological utility.

To address this problem, a number of different approaches for purifying CNTs have been developed in the past two decades. These include density gradient ultracentrifugation,[8] polymer wrapping,[9] DNA binding,[10] and chromatography.[11] Of these, polymer sorting has emerged as a particularly attractive strategy, offering high selectivity (>99%) and yield (>20%), as well as low cost and scalability.[12–14] A typical polymer sorting scheme involves ultrasonication of CNTs and sorting polymer

in an organic solvent, followed by selective precipitation of metallic CNTs via centrifugation, yielding a liquid dispersion of semiconducting CNTs. As such, polymer-sorted CNTS are highly amenable to solution-based deposition techniques such as inkjet printing,[15] solution soaking,[16] and spin-coating.[17] In most cases, however, the polymer remains bound to the CNTs after deposition. This results in devices with poor electrical performance, namely, high contact resistance, low mobility, and low on–off ratio.[18–20] Removing the polymer to recover the pristine electronic properties of the CNTs is therefore a necessary step to achieving high-performance CNT electronics based on polymer sorting.

Two main strategies have been established on this front. Removing the sorting polymer prior to deposition represents the most ideal approach, though this was found to produce unstable CNT dispersions, leading to CNT bundling and loss of semiconducting behavior.[20] Recent efforts have thus focused on removing the sorting polymer after CNT deposition. Examples include degradation of the sorting polymer by acid[21] or heat,[22] reversible depolymerization of metal-coordination polymers[23] or supramolecular polymers,[24] actuated changes in polymer conformation,[25] and targeted metal chelation.[18] However, designing polymers that are removable as well as effective at sorting CNTs is synthetically challenging. Furthermore, as many of these approaches exploit specific polymer chemistries, they cannot be generalized to other systems.

Recently, Yu et al. showed that partial removal of the sorting polymer can lead to improved device performance.[19] Specifically, there can be significant amounts of unbound sorting polymer present in polymer-sorted CNT films, in addition to the polymer bound to individual CNTs. This arises from the fact that maximal CNT sorting yields are typically achieved under polymer-rich conditions (e.g., polymer/CNT ratio > 1).[16,21,26] Consequently, excess unbound polymer is almost always present in polymer-sorted CNT dispersions. By filtering sorted CNT dispersions prior to CNT deposition, it is possible to separate the sorted CNTs from the excess polymer. It was revealed that this strategy resulted in CNT transistors with lower contact resistance and higher current density.[19] The filtered sorting polymer can also be recycled for further CNT purification. However, the filtered CNTs had to be redispersed in chloroform instead of toluene, the solvent originally used for sorting. This is likely due to the fact that too much excess polymer had been removed, making it difficult to redisperse the CNTs in toluene, a less toxic

T. Z. Gao
Department of Materials Science & Engineering
Stanford University
496 Lomita Mall, Stanford, CA 94305, USA
Dr. T. Lei, Dr. F. Molina-Lopez, Prof. Z. Bao
Department of Chemical Engineering
Stanford University
443 Via Ortega, Stanford, CA 94305, USA
E-mail: zbao@stanford.edu

The ORCID identification number(s) for the author(s) of this article can be found under https://doi.org/10.1002/smtd.201800189.

solvent with poor CNT solubility. Moreover, filtered CNTs must be redispersed using ultrasonication, a process that is known to damage CNTs.[27–29] Thus, in the interest of greener processing and high-performance CNT devices, a solution-based process that reduces the polymer/CNT ratio is highly desired.

Flocculation, the process of destabilizing a colloid by introduction of a flocculating agent, has been demonstrated to be an effective method for controlling the polymer content of polymer-stabilized graphene dispersions. Notably, Secor et al. were able to decrease the polymer/graphene ratio from ≈100 to ≈7 for graphene dispersions stabilized by cellulose derivatives.[30,31] Flocculation has also been applied to CNTs by Rogers and co-workers, but only as a way of controlling CNT deposition.[32,33] Here we utilize flocculation to lower the polymer/CNT ratio of CNT dispersions. This method substantially reduces the amount of excess sorting polymer in CNT dispersions and facilitates recycling of the sorting polymer. Additionally, this technique enhances process compatibility by eliminating the need for acid-based polymer degradation strategies while maintaining dispersibility in toluene. Furthermore, transistors made with flocculated CNTs exhibit significant improvements in device metrics such as mobility and on–off ratio.

2. Results and Discussion

2.1. Flocculation and Characterization

Sorted CNT dispersions were prepared using poly[(9,9-di-*n*-dodecyl-2,7-fluorendiyl-dimethine)-(1,4-phenylene-dinitrilomethine)] (PF-PD) as previously described by our group.[21] Small amounts of acetone were then added to these dispersions, inducing flocculation of the polymer-wrapped CNTs. After a short centrifugation step, the dispersion separated into two phases—a polymer-rich supernatant and a CNT floc. Unlike precipitation-based approaches, which produce a mass of bundled CNTs, the CNT floc is loosely held together, thus allowing for redispersion without ultrasonication. The supernatant was carefully decanted for recycling of the sorting polymer, while the floc was redispersed in toluene to produce a CNT dispersion with less excess polymer. These dispersions will hereafter be referred to as flocculated CNT dispersions. A schematic of this process is shown in **Figure 1**.

We first used spectroscopic techniques to determine the efficacy of flocculation. As PF-PD contains an imine moiety, the N 1s X-ray photoelectron spectroscopy (XPS) peak is sensitive to the amount of sorting polymer present. Flocculated and unflocculated CNTs were deposited on SiO_2 by dropcasting, and then analyzed by XPS. **Figure 2**a shows the N 1s XPS spectra normalized to C 1s peak intensity for both samples. The N 1s peak is present for unflocculated CNTs but cannot be observed in flocculated CNTs, suggesting a significant reduction in polymer content after flocculation.

This observation is also supported by UV–vis–NIR spectroscopy. Figure 2b shows the UV–vis–NIR spectra of flocculated and unflocculated CNT dispersions normalized to the peak at ≈950 nm, which arises from the CNT S22 transition. After flocculation, the absorbance peak at ≈400 nm from the sorting polymer is greatly decreased, indicating a reduction in the polymer concentration. To quantify the amount of acetone needed for flocculation to occur, different amounts of acetone were used, ranging from 10% to 50% v/v. Figure 2c shows the ratio of polymer and CNT absorbance as a function of acetone amount. We found that the flocculation process removed up to 95% of the excess polymer, as the polymer/CNT absorbance ratio can be reduced from ≈40 to ≈1. Furthermore, this ratio can be tuned within a certain range, ≈1–5, by the amount of acetone used during the flocculation process. Values higher than 5 were not achieved, as flocculation did not produce cohesive flocs for acetone amounts less than 25% v/v. Higher polymer/CNT ratios can potentially be achieved via alternative flocculants.

Having determined that flocculation can be used to lower the excess polymer content of CNT dispersions, we proceeded to study the flocculation process. To characterize how much excess polymer is removed during a single flocculation step, we performed sequential flocculation steps on the same CNT dispersion. After the first flocculation step, the CNT floc was redispersed in toluene and flocculated again. UV–vis–NIR spectroscopy was performed on the supernatant from each flocculation step, illustrated in **Figure 3**a. The intensity of the polymer absorbance peak at ≈400 nm was reduced from ≈5.5 after the first flocculation step to ≈0.1 after the second flocculation step, indicating that most of the excess polymer is removed by the first flocculation step.

We also found that flocculation can be used to prepare concentrated CNT dispersions. Under experimental conditions that maximize sorting yield, the concentration of PF-PD-sorted CNTs is typically around 10 µg mL^{-1}.[21] Higher concentrations can be obtained by utilizing more raw material during the sorting procedure, but with a decreased sorting yield. The CNT floc, however, can be redispersed at various concentrations without compromising the sorting yield, as shown in Figure 3b. This is highly advantageous for deposition techniques such as blade coating, wherein a specific concentration is required to
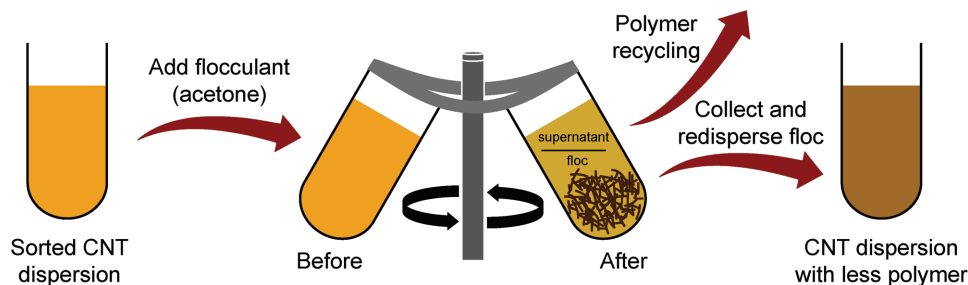

Figure 1. Schematic overview of flocculation.

ADVANCED
SCIENCE NEWS
www.advancedsciencenews.com
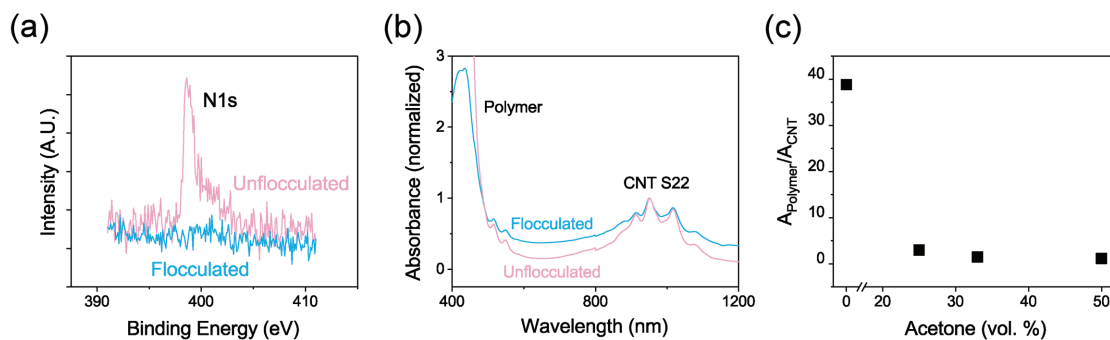
small
methods
www.small-methods.com

Figure 2. Spectroscopic characterization of flocculated CNTs. a) XPS N 1s spectra of flocculated and unflocculated CNTs. The N 1s peak arises from the imine moiety on the sorting polymer. b) UV–vis–NIR spectra of flocculated and unflocculated CNT dispersions in toluene. The concentration of CNTs in these dispersions is around 10 µg mL^{-1}. c) Ratio of polymer and CNT absorbance as a function of acetone amount.

achieve the target film thickness. Similarly, high concentrations are needed for technologies such as inkjet printing, as the number of printing passes is typically minimized for increased throughput. Later, we leverage this characteristic to fabricate high-performance, inkjet-printed CNT transistors with just 10 printing passes. Additionally, we compare the transistor performance of flocculated and unflocculated CNTs with the same deposition conditions and CNT concentrations.

Atomic force microscopy (AFM) was performed to determine whether flocculation affected the length distribution of CNTs. However, as illustrated in Figure 3c, flocculation did not cause notable changes in the length histogram. This indicates that the flocculation process only affects the amount of polymer in the dispersion and does not physically alter the CNTs.

Though removing excess polymer is beneficial for process integration and device performance, some excess polymer is needed to stabilize the dispersion in toluene.[19] Flocculating with a high amount of acetone was found to promote CNT aggregation, akin to complete polymer removal prior to deposition. Figure 3d shows the UV–vis–NIR spectra of dispersions flocculated with different amounts of acetone, normalized to the CNT S22 peak intensity. We note that there is considerable peak broadening for the sample flocculated with 33% acetone. Correspondingly, this sample also has the lowest polymer/CNT ratio. Minimal broadening was observed for the sample flocculated with 25% acetone. As peak broadening is related to CNT aggregation, this result reveals that aggregation can occur when too much excess polymer is removed. Carefully selecting
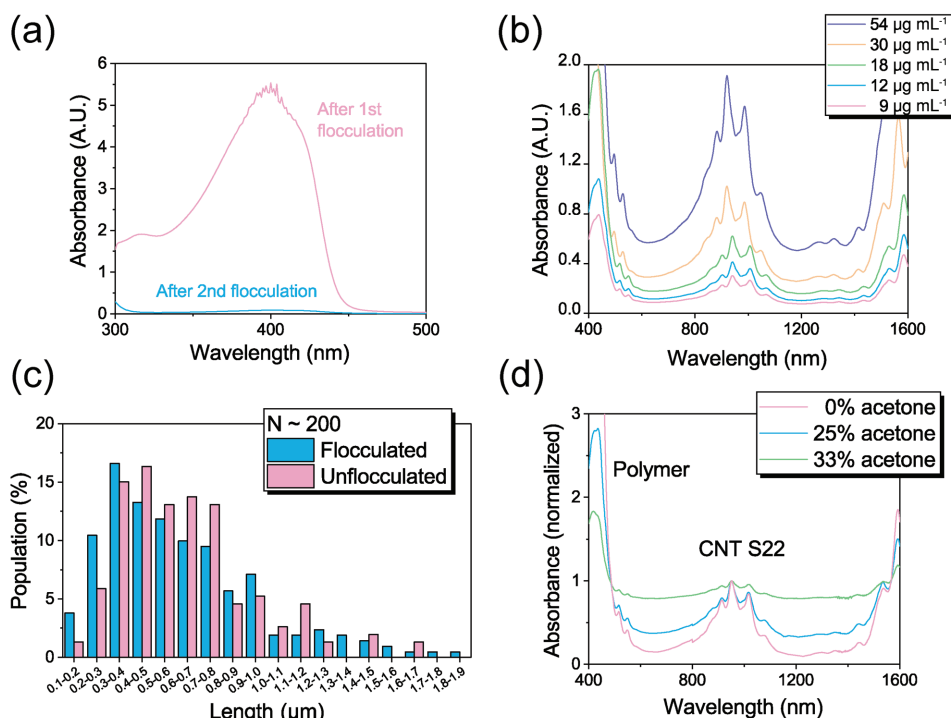

Figure 3. Flocculation process characterization. a) UV–vis–NIR spectra of extracted supernatant after multiple flocculation steps. The peak at 400 nm is from the conjugated polymer used for sorting. b) Flocculated CNTs redispersed in toluene at various concentrations. c) AFM histogram of CNT lengths before and after flocculation. d) UV–vis–NIR spectra showing signal broadening due to flocculation-induced CNT bundling.
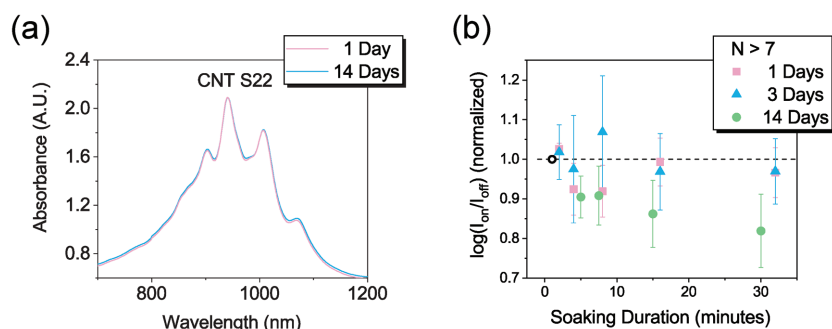
Figure 4. Stability of flocculated CNT dispersions. a) Shape of CNT S22 peak from UV–vis–NIR spectra as a function of elapsed time. b) On–off ratio as a function of soaking duration and elapsed time.

the amount of acetone used during the flocculation process is therefore crucial to obtaining well-dispersed CNT dispersions with less excess polymer. Results hereinafter were obtained with CNTs flocculated with 25% v/v acetone.

To further understand the stability of flocculated CNT dispersions, we monitored the UV–vis–NIR spectra of flocculated CNT dispersions over time. Broadening of CNT absorption peaks accompanied by decreasing intensity would indicate the formation of CNT bundles. As illustrated in **Figure 4**a, there is little change in the lineshape of the CNT S22 peak over a period of 14 days. This suggests that the CNTs are well dispersed and have not undergone significant aggregation. However, as device behavior is highly sensitive to the presence of metallic CNT bundles, more detailed device measurements were carried out to verify this conclusion. In particular, we characterized the on–off ratio of CNT transistors as a function of CNT deposition. Assuming that bundles are present in the dispersion, the probability of depositing a metallic CNT bundle increases as more CNTs are deposited. An on–off ratio that decreases with increasing deposition time is thus indicative of CNT bundles.

To test this, we fabricated bottom-contact transistors by solution soaking (see the Experimental Section for details). In this process, plasma-treated Si wafers with pre-patterned source and drain electrodes are directly immersed in a CNT dispersion, causing CNT deposition on the surface over time. Pd/Cr were used as electrodes, and 300 nm of SiO_2 as the dielectric. The channel width and W/L ratio were fixed at 50 µm and 20, respectively. CNT deposition durations ranged from 1 to 32 min. As shown in Figure 4b, there is no significant variation in the on–off ratio within the first 3 days after flocculation—the on–off ratio after 32 min of deposition is the same as the on–off ratio after 1 min of deposition. Fourteen days after flocculation, however, there is a considerable drop in the on–off ratio as soaking duration increases, indicating that CNT bundles have deposited in the channel. This suggests that flocculated CNT dispersions are stable on the timescale of days, but not weeks. Based on the UV–vis–NIR spectra, it is likely that only a small percentage of CNTs have formed bundles, leading to a largely unchanged spectroscopic lineshape.

To investigate the effect of flocculation on CNT network morphology, films of flocculated and unflocculated CNTs were deposited onto SiO_2 by inkjet printing as well as solution soaking. The concentration of CNTs (30 µg mL^{-1}), number of printing passes (10 layers), and soaking duration (5 min) were kept constant

across all samples. AFM was used to image the as-deposited films, but only yielded images of polymer, rather than CNTs. The films were subsequently washed to dissolve away excess polymer from the surface. Prior reports have utilized small amounts of acid during the washing step to break apart the sorting polymer.[21,24] This strategy was employed to great effect for PF-PD-wrapped plasma discharge CNTs, with notable increases in device metrics such as mobility and on–off ratio after washing with trifluoroacetic acid (TFA).[21] However, due to the reduction in excess polymer content after flocculation, we found that washing with toluene was sufficient for producing polymer-free CNT networks. This can be seen in **Figure 5**, which compares the morphology of flocculated and unflocculated CNT films after washing with toluene. Figure 5a,c exhibits pristine CNT networks consistent with polymer removal via flocculation. Figure 5b, on the other hand, reveals the presence of polymer residue throughout the film, while Figure 5d shows some polymer residue in the bottom left corner of the AFM scan. Eliminating the need for acid-based washing enhances CNT process integration, as many materials and processes are sensitive to acid. Moreover, TFA is known to dope CNTs, which can compromise the performance of CNT-based devices.[20]

Figure 5 also demonstrates that flocculation can improve CNT network density. Figure 5a,b shows inkjet-printed films of flocculated and unflocculated CNTs prepared with the same printing parameters. The flocculated CNT film exhibits a much higher CNT density, which we attribute to the stochastic nature of inkjet printing. As droplets containing CNTs and excess polymer are deposited onto the substrate, CNTs come into direct contact with the substrate in some areas. In other areas, however, polymer comes into contact with the surface first, resulting in a thin layer of polymer forming between CNTs and the substrate. Consequently, during the washing step, this thin layer is dissolved, delaminating the CNTs above. For flocculated CNTs, on the other hand, most of the CNTs are able to interact directly with the substrate without being screened by excess polymer. Thus, less CNTs are removed by the washing process, yielding a network of higher density compared to unflocculated CNTs.

Figure 5c,d reveals that CNT density can also be increased via flocculation for solution soaking, though to a lesser extent. We believe that this arises from the electrostatic interaction between CNTs and the substrate, which is much stronger than the interaction between excess polymer and the substrate. CNTs can therefore skirt around excess polymer during the solution-soaking process, allowing CNTs to adhere to the substrate irrespective of excess polymer in the dispersion. However, similar to inkjet-printed films, soaking with flocculated CNTs leads to cleaner CNT networks, as evidenced by the polymer still present in the bottom left corner of Figure 5d.

2.2. Device Fabrication and Characterization

The above work using spectroscopy and AFM demonstrated that flocculation lowers the polymer/CNT ratio. The ensuing
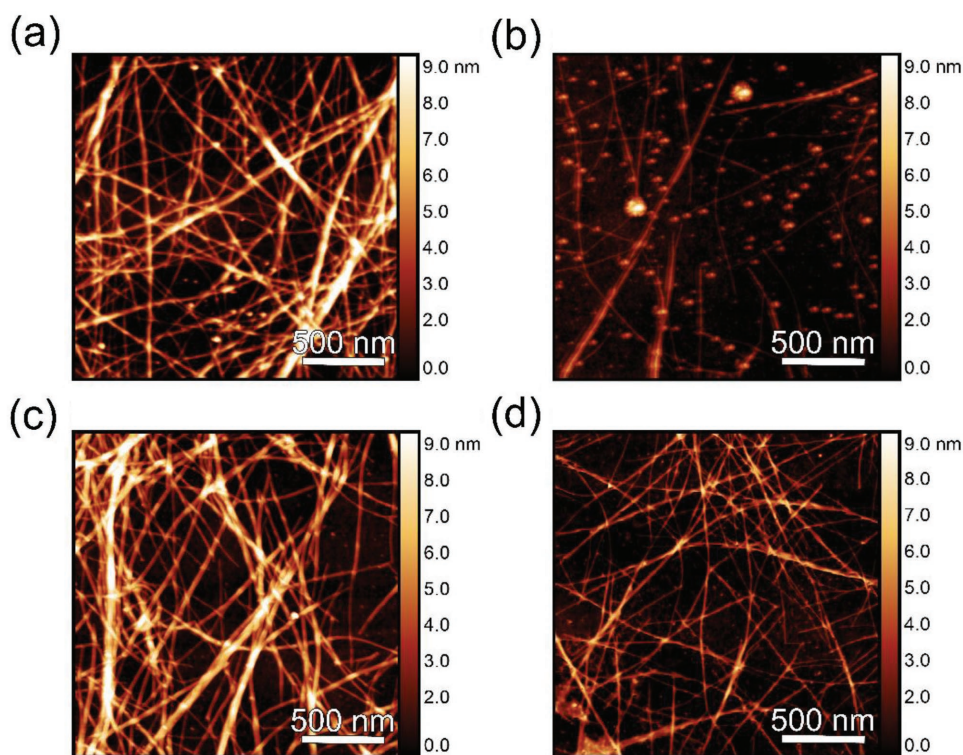
ADVANCED
SCIENCE NEWS
www.advancedsciencenews.com

small
methods
www.small-methods.com

Figure 5. Representative AFM scans of flocculated and unflocculated CNT films deposited by inkjet printing and solution soaking. a) Flocculated, inkjet. b) Unflocculated, inkjet. c) Flocculated, soaking. d) Unflocculated, soaking.

dispersion is stable on the timescale of days and can be concentrated for efficient deposition. Additionally, this process does not compromise sorting yield or CNT length distribution, while also enabling higher CNT network density by preventing delamination during washing steps. Next, we compare the performance of CNT devices with and without flocculation to understand the effect of flocculation on device performance. Bottom-contact transistors were prepared using inkjet printing as well as solution soaking following the procedure described above. These devices were then washed with toluene, and subsequently measured at a V_{GS} of −40 V to quantify the yield. A working device is defined as having an on–off ratio above 10^2. Devices with a large quantity of polymer present in the channel are expected to have poor electrical transport, and therefore possess a low on–off ratio. The device yield can thus be used as an indicator of the presence of polymer within the CNT network. As seen in **Figure 6**a, flocculation leads to a substantial increase in device yield for inkjet-printed devices. This is likely to be related to delamination. Unflocculated, inkjet-printed CNT films are highly susceptible to delamination due to their nonuniform morphology, resulting in CNT networks near or below the percolation threshold, which manifests as a low device yield. For solution soaking, on the other hand, a high device yield is observed for both flocculated and unflocculated CNTs. This is consistent with our hypothesis that CNTs can skirt around the excess polymer during the solution-soaking process, yielding percolative CNT networks regardless of the excess polymer content.

These observations are supplemented by on-current measurements, illustrated in Figure 6b. The on-current depends on gating efficiency and conductance of the channel, which is dictated by the presence of excess polymer as well as CNT network morphology. For unflocculated CNTs, treatment with TFA is necessary to achieve maximal on-current, indicating that charge transport is being impeded by excess polymer. For flocculated CNTs, on the other hand, using TFA does not lead to a significant improvement in on-current, indicating that the polymer content in flocculated CNT films is low enough to not impede charge transport. The on-current of inkjet-printed transistors is observed to be lower than those made by solution soaking across the board. We attribute this to differences in CNT film thickness. Ten layers of inkjet printing and 5 min of solution soaking resulted in films with an average thickness of 79 ± 18 nm and 279 ± 87 nm, respectively. Attempts to fabricate thick films via inkjet printing produced transistors with low on–off ratios ($<10^4$), precluding a thickness-independent comparison of these two deposition methods.

We also investigated the effect of flocculation on device metrics such as on–off ratio and mobility. Figure 6c shows mobility versus on–off ratio for inkjet-printed devices, while Figure 6d shows the same for devices made by solution soaking. The top right corner of the plot represents the most desirable region, i.e., devices with both high mobility and on–off ratio. Both plots demonstrate that flocculation leads to a substantial improvement in device performance—charge transport becomes more efficient as excess polymer is removed from the film. Notably, the mobility for inkjet-printed transistors washed with toluene increases from ≈0.1 to over 10 cm^2 V^{-1} s^{-1}. Moreover, the performance of inkjet-printed, flocculated CNT transistors (mobility ≈11 cm^2 V^{-1} s^{-1}, $I_{on}/I_{off} \approx 10^6$) is comparable to that
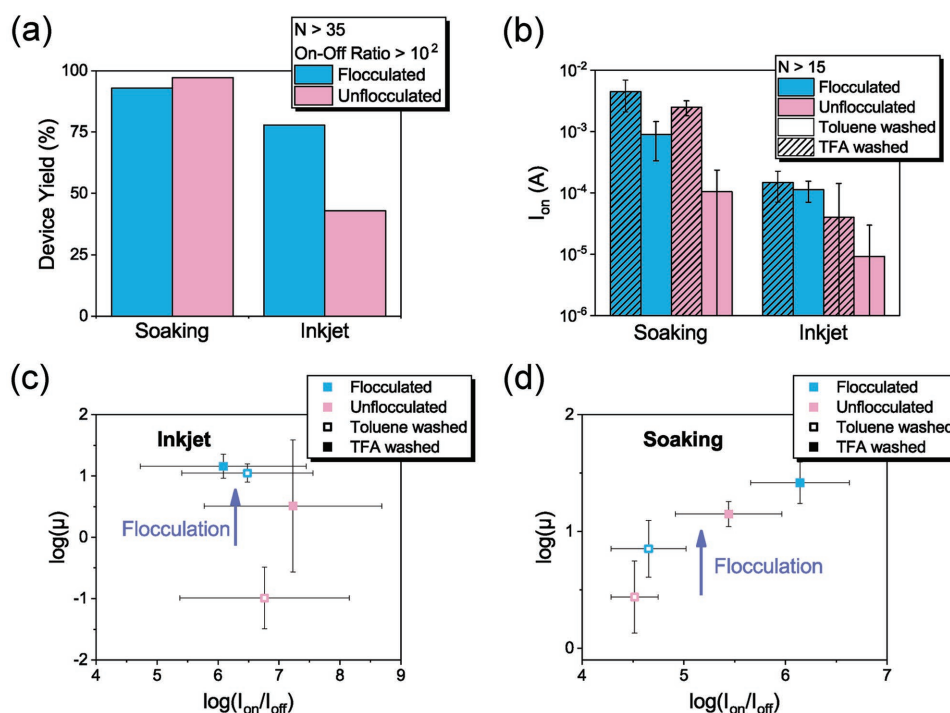
Figure 6. Electronic characterization of flocculated CNTs. a) Device yield after toluene wash. Working devices were defined as having on–off ratios above 10^2. b) On-current comparison. c,d) Figures of merit for devices made by (c) inkjet printing (d) and soaking.

of TFA-washed devices made by solution soaking and unflocculated CNTs (mobility ≈ 12 cm^2 V^{-1} s^{-1}, $I_{on}/I_{off} \approx 10^{5.5}$). This result highlights the promise of flocculation, as inkjet-printed devices typically possess lower performance than devices made by solution soaking in exchange for greater patterning versatility.

Our prior observations suggest that flocculation removes most of the excess polymer, eliminating the need for a TFA wash. However, for solution-soaked devices made with flocculated CNTs, washing with TFA was still found to improve mobility and on–off ratio, as shown in Figure 6d. If most of the polymer is indeed removed by flocculation, one would expect little change in performance after a TFA wash, as we observed for the inkjet-printed devices in Figure 6c. This may be due to polymer being trapped within the CNT network during the soaking process. The trapped polymer must be broken down by TFA before it can be washed away. Inkjet-printed films, on the other hand, are much less uniform than their solution-soaking counterparts. Excess polymer in these films is less tightly trapped within the CNT network, and can be easily removed by washing with toluene. For both deposition methods, devices made with unflocculated CNTs improve drastically upon exposure to TFA as expected.

The effect of flocculation on the electrical performance of CNT transistors is further illustrated by the transfer curves in **Figures 7**a,b. Transistors fabricated with flocculated CNTs exhibit less variation in transfer characteristics across devices. Unflocculated CNTs, on the other hand, show high variance across devices. This is attributed to the stochastic nature of inkjet printing combined with high amounts of excess polymer. For devices made by solution soaking, flocculation has little effect on the uniformity of the transfer curves,

confirming that this deposition method is less sensitive to the CNT–polymer ratio as we postulated.

Finally, we apply this method to other sorting polymers to validate the versatility of this approach. **Figure 8**a shows the polymers we investigated. Both poly(3-dodecylthiophene) (P3DDT) and PF-PD are conjugated polymers, while polymer 1 is a supramolecular polymer. CNT sorting was performed with each of these three polymers with plasma discharge CNTs in toluene. The ensuing dispersions were then flocculated with acetone. As demonstrated in Figure 8b, PF-PD is the most sensitive to acetone, with a $\approx 90\%$ reduction in polymer content after flocculation, while P3DDT is the least sensitive, showing only $\approx 25\%$ reduction. XPS was also performed to compare flocculated and unflocculated CNTs. Both PF-PD and polymer 1 contain nitrogen moieties, while P3DDT contains sulfur, so N/C and S/C were used as the respective metrics. Again, PF-PD appears to be the most sensitive to flocculation with acetone, with almost no detectable nitrogen content after flocculation, whereas both P3DDT and polymer 1 exhibit some decrease in polymer content. These results reveal that flocculation can be applied generally to polymer-sorted CNTs, and that the efficacy of flocculation for each system will depend on the details of the polymer–flocculant interaction.

The applicability of this strategy to other sorting polymers also enables recycling of polymers that are not reversibly polymerizable. The majority of reported recyclable sorting polymers are recycled by depolymerization followed by resynthesis from monomers. Flocculation, on the other hand, allows for a substantial portion of the excess sorting polymer to be extracted via the polymer-rich supernatant. After evaporation of the flocculant, the sorting polymer is recovered without the
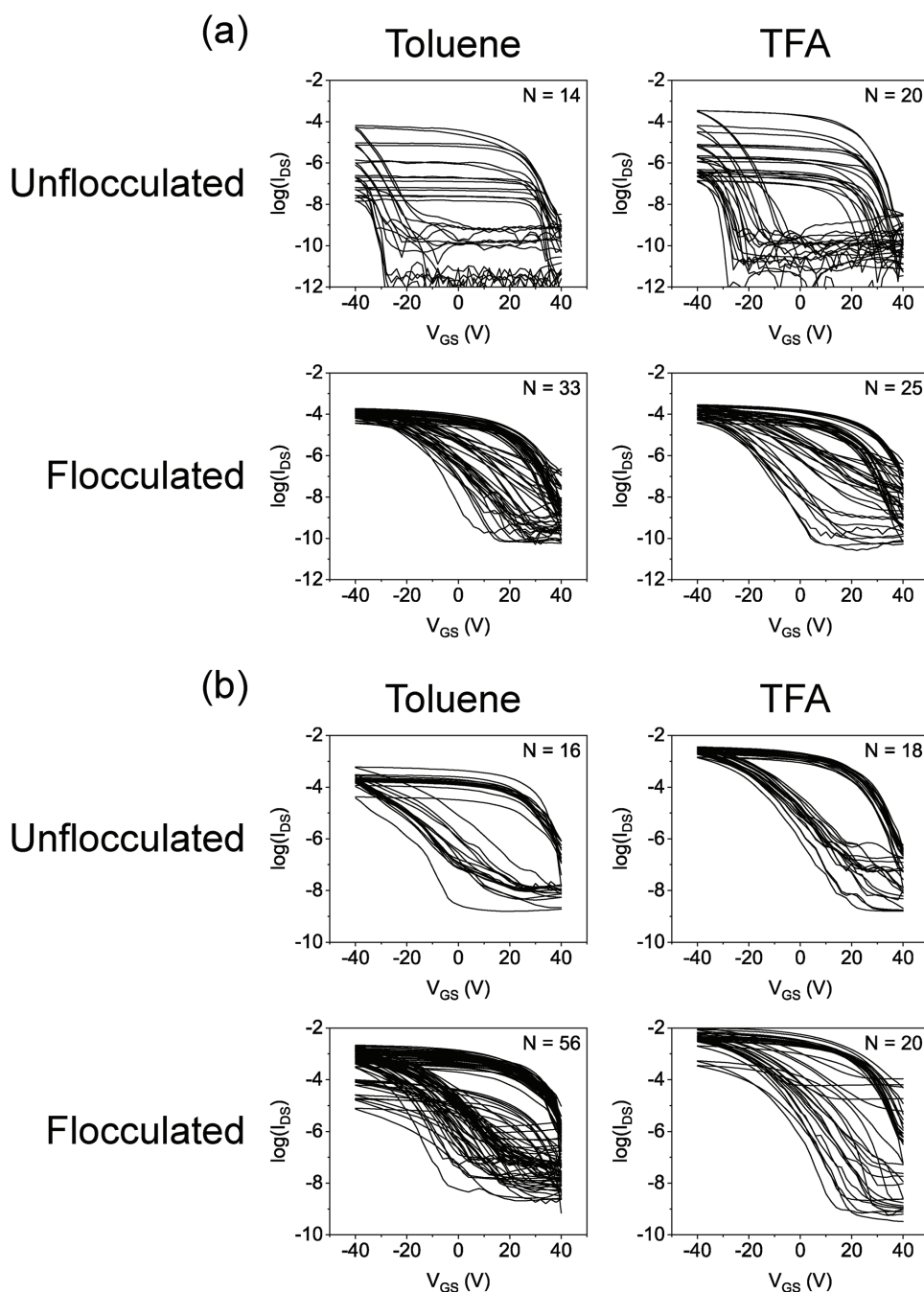
(a)

Figure 7. Transfer characteristics of CNT transistors made by a) inkjet printing and b) solution soaking.

need for resynthesis. This approach can potentially be applied to all sorting polymers, given that an effective flocculant is identified.

3. Conclusion

In summary, we developed a technique for reducing excess polymer content in polymer-sorted CNT dispersions based on flocculation. This strategy can be applied to a range of sorting polymers, including conjugated and supramolecular polymers, as well as different deposition techniques, such as inkjet printing and solution soaking. We found that flocculation enables the deposition of higher density CNT films, while also increasing the device yield, mobility, and on–off ratio. Moreover, flocculation eliminates the need for acid-based washing steps and facilitates recycling of the polymer, enhancing process compatibility and versatility. Flocculation was observed to be particularly effective for inkjet-printed CNT transistors, producing devices with mobilities ≈ 10 cm^2 V^{-1} s^{-1} and on–off ratios $\approx 10^6$ on SiO$_2$. These values are comparable to TFA-washed devices made by solution soaking, but with the additional patterning
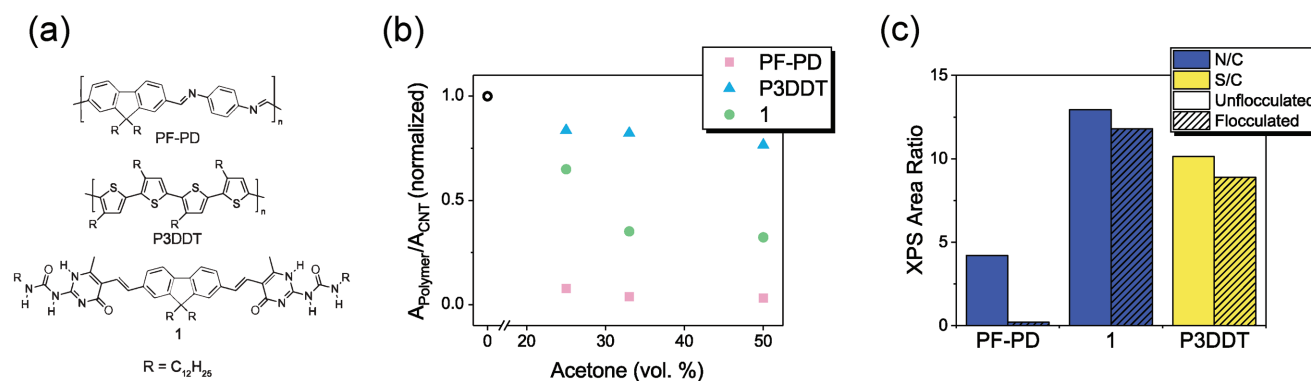
Figure 8. Extension of flocculation to other sorting polymers. a) Chemical structure of PF-PD, P3DDT, and polymer 1. b) Normalized polymer–CNT absorbance ratio as a function of acetone amount for the polymers shown in (a). c) XPS area ratios of N/C and S/C before and after flocculation for the polymers shown in (a).

versatility of inkjet printing. Thus, flocculation is a facile, solution-based method for improving the process integration and device performance of polymer-sorted CNTs.

4. Experimental Section

Preparation of CNT Dispersions: The procedures for CNT sorting were taken from refs. [16,21,24]. In brief, plasma discharge CNTs (Raymor Industries Inc., RN-020) and sorting polymer were mixed with 25 mL of toluene, and then sonicated for 30 min (Cole-Parmer 750-Watt Ultrasonicator). Sonication powers for PF-PD, P3DDT (Sigma-Aldrich), and polymer 1 were 45%, 30%, and 70%, respectively. A dry ice/acetone bath was used to cool the sample during sonication. After sonication, the dispersion was centrifuged at 8000 rpm for 5 min, followed by centrifugation at 17000 rpm for 25 min (Sorvall LYNX 4000). In both steps, the pellet was discarded. Typical mass loadings were 10–15 mg for CNTs and 5–10 mg for the sorting polymer. All dispersions were stored at 4 °C to prevent aggregation. For flocculated dispersions, acetone was added to the sorted CNT dispersions, and subsequently centrifuged at 17000 rpm for 10 min. The supernatant was carefully decanted, and the floc was then redispersed in toluene.

Characterization of Flocculated CNTs: CNT and sorting polymer absorbance was measured by UV–vis–NIR spectroscopy (Cary 6000i) with 1 cm path length quartz cuvettes and toluene as the background. CNT concentrations were estimated using a calibration curve as described by Lei et al.[21] Typical values were in the range of 10–30 µg mL^{-1}, depending on the mass loading of polymer and CNTs. AFM images were obtained using a Veeco AFM in tapping mode under ambient conditions. XPS was performed using a PHI VersaProbe I.

CNT Transistor Fabrication: Source–drain electrodes were defined on 300 nm SiO$_2$ wafers by photolithography. 2 nm of Cr and 40 nm of Pd electrodes were thermally evaporated as the bottom contacts, followed by a lift-off process in acetone. These wafers were treated by O$_2$ plasma for 30 s at 150 W prior to CNT deposition. For devices prepared by solution soaking, the wafers were directly immersed in the CNT dispersion for up to 32 min. Inkjet-printed devices were fabricated using a Dimatix Material Printer DMP-2831 with 10 pL droplet size cartridges. Tetralin (2.5% v/v) was added to CNT dispersions prior to printing to improve the wetting behavior. The printer parameters were as follows: 25 °C substrate and printhead temperature, 5 in. H$_2$O meniscus vacuum point, 35 µm drop-to-drop spacing, 4 nozzles, 10 passes, and ≈25 V applied during jetting.

Device Post-Processing and Measurement: Following CNT deposition, devices were washed by immersion in toluene or a 1% TFA/toluene mixture for 5 min and annealed for 10 min at 90 °C. Afterwards, the devices were annealed under vacuum for 30 min at 150 °C to de-dope the CNTs. For devices prepared by solution soaking, additional photolithography and O$_2$ plasma steps were used to remove CNTs outside of the channel.

Transistor measurements were performed in ambient conditions using a Keithley 4200 SCS. Mobility was calculated in the saturation regime from the slope of the $I_{ds}^{1/2}$–V_{gs} plot using the following equation:

$$\frac{\partial \sqrt{I_{ds}}}{\partial V_{gs}} = \sqrt{\frac{\mu W C}{2L}}$$

where W and L are the width and length of the channel, respectively, and C is the parallel plate gate capacitance for 300 nm of SiO$_2$. For 1D materials such as CNTs, the parallel plate model is known to underestimate the gate capacitance due to limited surface coverage.[34,35] The mobility of CNT transistors calculated using this model may therefore be higher than reported.

Conflict of Interest

The authors declare no conflict of interest.

[1] D. Zhong, Z. Zhang, L.-M. Peng, *Nanotechnology* **2017**, *28*, 212001.
[2] Y. Cao, S. Cong, X. Cao, F. Wu, Q. Liu, M. R. Amer, C. Zhou, *Top. Curr. Chem.* **2017**, *375*, https://doi.org/10.1007/s41061-017-0160-5.

[3] J. Zhu, M. C. Hersam, *Adv. Mater.* **2017**, *29*, https://doi.org/10.1002/adma.201603895.

[4] K. Chen, W. Gao, S. Emaminejad, D. Kiriya, H. Ota, H. Y. Y. Nyein, K. Takei, A. Javey, *Adv. Mater.* **2016**, *28*, 4397.

[5] A. E. Islam, J. A. Rogers, M. A. Alam, *Adv. Mater.* **2015**, *27*, 7908.

[6] L. Cai, C. Wang, *Nanoscale Res. Lett.* **2015**, *10*, https://doi.org/10.1186/s11671-015-1013-1.

[7] G. S. Tulevski, A. D. Franklin, D. Frank, J. M. Lobez, Q. Cao, H. Park, A. Afzali, S.-J. Han, J. B. Hannon, W. Haensch, *ACS Nano* **2014**, *8*, 8730.

[8] M. S. Arnold, A. A. Green, J. F. Hulvat, S. I. Stupp, M. C. Hersam, *Nat. Nanotechnol.* **2006**, *1*, 60.

[9] A. Nish, J.-Y. Hwang, J. Doig, R. J. Nicholas, *Nat. Nanotechnol.* **2007**, *2*, 640.

[10] X. Tu, S. Manohar, A. Jagota, M. Zheng, *Nature* **2009**, *460*, 250.

[11] H. Liu, D. Nishide, T. Tanaka, H. Kataura, *Nat. Commun.* **2011**, *2*, 309.

[12] T. Lei, I. Pochorovski, Z. Bao, *Acc. Chem. Res.* **2017**, *50*, 1096.

[13] J. Lefebvre, J. Ding, Z. Li, P. Finnie, G. Lopinski, P. R. L. Malenfant, *Acc. Chem. Res.* **2017**, *50*, 2479.

[14] H. Wang, Z. Bao, *Nano Today* **2015**, *10*, 737.

[15] C. M. Homenick, R. James, G. P. Lopinski, J. Dunford, J. Sun, H. Park, Y. Jung, G. Cho, P. R. L. Malenfant, *ACS Appl. Mater. Interfaces* **2016**, *8*, 27900.

[16] H. W. Lee, Y. Yoon, S. Park, J. H. Oh, S. Hong, L. S. Liyanage, H. Wang, S. Morishita, N. Patil, Y. J. Park, J. J. Park, A. Spakowitz, G. Galli, F. Gygi, P. H.-S. Wong, J. B.-H. Tok, J. M. Kim, Z. Bao, *Nat. Commun.* **2011**, *2*, 541.

[17] A. Chortos, G. I. Koleilat, R. Pfattner, D. Kong, P. Lin, R. Nur, T. Lei, H. Wang, N. Liu, Y.-C. Lai, M.-G. Kim, J. W. Chung, S. Lee, Z. Bao, *Adv. Mater.* **2016**, *28*, 4441.

[18] Y. Joo, G. J. Brady, C. Kanimozhi, J. Ko, M. J. Shea, M. T. Strand, M. S. Arnold, P. Gopalan, *ACS Appl. Mater. Interfaces* **2017**, *9*, 28859.

[19] X. Yu, D. Liu, L. Kang, Y. Yang, X. Zhang, Q. Lv, S. Qiu, H. Jin, Q. Song, J. Zhang, Q. Li, *ACS Appl. Mater. Interfaces* **2017**, *9*, 15719.

[20] B. Norton-Baker, R. Ihly, I. E. Gould, A. D. Avery, Z. R. Owczarczyk, A. J. Ferguson, J. L. Blackburn, *ACS Energy Lett.* **2016**, *1*, 1212.

[21] T. Lei, X. Chen, G. Pitner, H.-S. P. Wong, Z. Bao, *J. Am. Chem. Soc.* **2016**, *138*, 802.

[22] Z. Li, J. Ding, C. Guo, J. Lefebvre, P. R. L. Malenfant, *Adv. Funct. Mater.* **2018**, *28*, 1705568.

[23] F. Toshimitsu, N. Nakashima, *Nat. Commun.* **2014**, *5*, 5041.

[24] I. Pochorovski, H. Wang, J. I. Feldblyum, X. Zhang, A. L. Antaris, Z. Bao, *J. Am. Chem. Soc.* **2015**, *137*, 4328.

[25] S. Liang, Y. Zhao, A. Adronov, *J. Am. Chem. Soc.* **2014**, *136*, 970.

[26] J. Ding, Z. Li, J. Lefebvre, F. Cheng, G. Dubey, S. Zou, P. Finnie, A. Hrdina, L. Scoles, G. P. Lopinski, C. T. Kingston, B. Simard, P. R. L. Malenfant, *Nanoscale* **2014**, *6*, 2328.

[27] A. Graf, Y. Zakharko, S. P. Schießl, C. Backes, M. Pfohl, B. S. Flavel, J. Zaumseil, *Carbon* **2016**, *105*, 593.

[28] F. Hennrich, R. Krupke, K. Arnold, J. A. Rojas Stütz, S. Lebedkin, T. Koch, T. Schimmel, M. M. Kappes, *J. Phys. Chem. B* **2007**, *111*, 1932.

[29] S. Mouri, Y. Miyauchi, K. Matsuda, *J. Phys. Chem. C* **2012**, *116*, 10282.

[30] E. B. Secor, P. L. Prabhumirashi, K. Puntambekar, M. L. Geier, M. C. Hersam, *J. Phys. Chem. Lett.* **2013**, *4*, 1347.

[31] E. B. Secor, T. Z. Gao, A. E. Islam, R. Rao, S. G. Wallace, J. Zhu, K. W. Putz, B. Maruyama, M. C. Hersam, *Chem. Mater.* **2017**, *29*, 2332.

[32] J.-U. Park, M. A. Meitl, S.-H. Hur, M. L. Usrey, M. S. Strano, P. J. A. Kenis, J. A. Rogers, *Angew. Chem., Int. Ed.* **2006**, *45*, 581.

[33] M. A. Meitl, Y. Zhou, A. Gaur, S. Jeon, M. L. Usrey, M. S. Strano, J. A. Rogers, *Nano Lett.* **2004**, *4*, 1643.

[34] Q. Cao, M. Xia, C. Kocabas, M. Shim, J. A. Rogers, S. V. Rotkin, *Appl. Phys. Lett.* **2007**, *90*, 023516.

[35] C. Wang, J.-C. Chien, K. Takei, T. Takahashi, J. Nah, A. M. Niknejad, A. Javey, *Nano Lett.* **2012**, *12*, 1527.